Available online at www.sciencedirect.com
ScienceDirect
Biochemical and Biophysical Research Communications 367 (2008) 826–833
BBRC
www.elsevier.com/locate/ybbrc

Caveolin-1 deficiency alters plasma lipid and lipoprotein profiles in mice

Susanne Heimerl [a,1], Gerhard Liebisch [a,1], Soazig Le Lay [b], Alfred Böttcher [a], Philipp Wiesner [a], Silke Lindtner [a], Teymuras V. Kurzchalia [b], Kai Simons [b], Gerd Schmitz [a,*]

[a] *Institute of Clinical Chemistry and Laboratory Medicine, University of Regensburg, Franz-Josef-Strauss-Allee 11, 93042 Regensburg, Germany*
[b] *Max Planck Institute of Molecular and Cellular Biology and Genetics, 01307 Dresden, Germany*

Received 2 January 2008
Available online 10 January 2008

Abstract

Caveolae are specialized membrane microdomains formed as the result of local accumulation of cholesterol, glycosphingolipids, and the structural protein caveolin-1 (Cav-1). To further elucidate the role of Cav-1 in lipid homeostasis *in-vivo*, we analyzed fasting and postprandial plasma from Cav-1 deficient mice on low or on high fat diet. In total plasma analysis, an increase in ceramide and hexosylceramide was observed. In cholesteryl ester (CE), we found an increased saturated + monounsaturated/polyunsaturated fatty acid ratio in fasting plasma of low fat fed Cav-1(−/−) mice with increased proportions of CE16:1, CE18:1, CE20:3, and decreased proportions of CE18:2 and CE22:6. Under high fat diet HDL-CE, free cholesterol and pre-β-HDL were increased accompanied by a shift from slow to fast migrating α-HDL and expansion of apoE containing HDL. Our results demonstrate a significant role of Cav-1 in HDL-cholesterol metabolism and may reflect a variety of Cav-1 functions including modulation of ACAT activity and SR-BI function.

Keywords: Caveolin-1; Caveolae; Lipid metabolism; HDL-cholesterol; Cholesterol ester

Caveolae are 50–100 nm invaginations of the plasma membrane that form specialized microdomains with localized accumulation of cholesterol and glycosphingolipids [1]. Caveolae are present in most cell types but are enriched in adipocytes, endothelial cells, and myocytes [1]. Caveolin-1 (Cav-1) is a marker protein selectively localized to caveolae that plays a pivotal role for caveolar function in intracellular trafficking and signal transduction [1–3]. Cav-1 is an integral membrane protein that can directly bind cholesterol thereby driving caveolae formation serving as a structural component of caveolae [3,4].

The important physiological role of Cav-1 and its family members Caveolin-2 and Caveolin-3 has been studied through the generation of various caveolin knockout animal models [5]. Cav-1 knockout mice exhibit a complete absence of caveolae in all Cav-1 expressing tissues while lack of caveolae in Cav-3 deficient mice is restricted to muscle tissues. Cav-2 deficient mice appear normal concerning the presence of caveolae [6–8]. The almost complete loss of caveolae in Cav-1 null mice results in various dysfunctions of mainly the lung and the vascular system [6,9,10].

Because of its high expression in adipose tissue, special attention has also been drawn on the role of Cav-1 in adipocytes and lipid metabolism. In adipocytes, Cav-1 is induced during adipogenesis [11] and can localize around lipid droplets [12]. Recently, an original caveolar endocytic trafficking pathway was identified linking plasma membrane caveolae to lipid droplets and influencing lipid sensing and storage in adipocytes [13]. Therefore, Cav-1 and caveolae have been suggested to cooperate with other proteins in the uptake and transport of fatty acids into lipid droplets which mainly consist of fatty acids and cholesteryl esters (CE) [1,12,14,15]. Cav-1 deficient mice are lean and show resistance to diet-induced obesity. Serum lipid analysis of Cav-1(−/−) mice revealed, in particular in a postprandial state under chow diet, strongly elevated levels of

* Corresponding author. Fax: +49 941 944 6202.
E-mail address: gerd.schmitz@klinik.uni-regensburg.de (G. Schmitz).
[1] These authors contributed equally to this work.

0006-291X/$ - see front matter © 2008 Elsevier Inc. All rights reserved.
doi:10.1016/j.bbrc.2008.01.010

triglyceride and free fatty acids related to an increased chylomicrons/very low density lipoprotein (VLDL) fraction and impaired clearance after oral fat load independent from lipoprotein lipase activity [16]. In contrast, no major alterations in serum HDL-cholesterol were observed [16].

However, the so far published data do only allow limited conclusion on the role Cav-1 in lipid and lipoprotein metabolism. In particular, the effect of Cav-1 deficiency on serum lipid and lipoprotein metabolism in response to a high fat diet has not been investigated so far. To further elucidate the role of Cav-1 in lipid metabolism, we here performed a detailed lipid and lipoprotein analysis of Cav-1(−/−) mice that were kept on low fat diet or challenged with a high fat diet and collected plasma samples in fasted and post-prandial state.

Materials and methods

Animals. Cav-1 deficient mice were described previously [17]. All animals used in these studies (mice homozygous null for the *caveolin-1* gene and their wild-type littermates) were of a C57BL/6 × sv129 genetic background and were genotyped by PCR, as previously described [17]. All animal experiments were approved by local authorities in accordance outlined by the American Physiological Society. Mice were kept on a 12-h light/dark cycle. After four weeks of weaning mice were put either on low fat diet (10% kcal% fat) or on high fat diet (60% kcal% fat) (Research Diets, New Brunswick, USA). Plasma samples were taken from 9-month-old mice. Fasting samples were taken after a fasting period of 14 h.

Lipid analysis by electrospray ionization tandem mass spectrometry (ESI-MS/MS). Lipids were quantified by ESI-MS/MS in positive ion mode (as described previously [18–21]). Samples were quantified by direct flow injection analysis using the analytical setup described by Liebisch et al. [21]. A precursor ion scan of *m/z* 184 specific for phosphocholine containing lipids was used for phosphatidylcholine, sphingomyelin [21], and lysophosphatidylcholine [20]. Ceramide was analyzed similar to a previously described methodology [19] using *N*-hepatadecaonyl-sphingosine as internal standard. Hexosylceramide was quantified in analogy. Free cholesterol and CE were quantified by a fragment ion of *m/z* 369 after selective derivatization of free cholesterol [22]. Quantification was achieved by calibration lines generated by addition of naturally occurring lipid species [19–22].

Lipoprotein separation with fast performance liquid chromatography (FPLC). Serum lipoproteins were isolated from mouse serum as previously described [23]. For this purpose, we used a Pharmacia Smart System® FPLC equipped with a Superose 6 PC 3.2/30 column. The elution was performed in Dulcobeco's PBS containing 1 mM EDTA as a running buffer. After loading 50 µl serum the system was run with a constant flow of 40 µl/min and fractionation was started after 18 min with 40 µl per fraction. Fractions 1–36 containing the serum lipoproteins were used for further analysis on a Cobas Integra 400 (Roche Diagnostic, Penzberg, Germany) to determine cholesterol and triglyceride levels of each fraction and for mass spectrometric analysis as described above. The cholesterol and triglyceride determination assays are standard enzymatic, colorimetric methods, which are also used in routine diagnostics (Roche Diagnostic).

Plasma agarose gel electrophoresis. One microliter of plasma was diluted to 4 µl with Tris–tricine buffer containing 10 glycerol and bromphenol blue and was separated in 0.7% (w/v) agarose (SeaKem® LE; FMC Bioproducts, Rockland, ME) gels in 25 mM Tris–tricine buffer (pH 8.6), containing 3 mM calcium lactate and 0.05% sodium azide. Gels were free of bovine serum albumin. Samples were electrophoresed at 100-V constant voltage and 10 °C for about 1 h, when the albumin stained with bromophenol blue had moved 4 cm.

Two-dimensional nondenaturing gradient gel electrophoresis. For the first dimension, 5 µl of plasma was separated in 0.7% (w/v) agarose (SeaKem® LE; FMC Bioproducts, Rockland, ME) gels in 50 mM barbital buffer (pH 8.6). Gels were free of bovine serum albumin. Samples were electrophoresed at 100-V constant voltage and 10 °C for about 1 h, when the albumin stained with bromophenol blue had moved 4 cm. For the second dimension, the agarose gel strips from the first dimension were transferred to a 4–15% polyacrylamide gradient gel (Ready gels; Bio-Rad, Munich, Germany). Separation in the second dimension was performed at 20 mA per gel for 4 h at 4 °C. Molecular weight standards (Pharmacia, Freiburg, Germany) containing thyroglobulin, 669 kDa; ferritin, 440 kDa; catalase, 232 kDa; lactate dehydrogenase, 140 kDa; and albumin, 67 kDa were run simultaneously with the sample.

Immunoblotting and chemiluminescence detection. After electrophoresis, proteins were electrophoretically transferred to Fluorotrans transfer membranes of 0.2-µm pore size (Pall, Dreieich, Germany). Transfer was carried out for 18 h in 20 mM Tris and 150 mM glycine buffer, in a *Trans*-Blot cell (Bio-Rad) at a constant 30 V and 10 °C. The lane with molecular weight standards was cut off and stained with Coomassie blue. Membranes were then blocked by incubation for 1 h in phosphate-buffered saline (PBS) containing 5% nonfat milk powder and 0.1% Tween-20. For the detection of the individual apolipoproteins, membranes were incubated for 1 h with the corresponding antibodies in a dilution of 1:5.000 in PBS with 1% nonfat milk powder and 0.1% Tween-20. The following antibodies were used: polyclonal rabbit anti-mouse apoAI and polyclonal rabbit anti-mouse apoE (Acris, Hiddenhausen, Germany).

After antibody incubation, the membrane was washed three times (10 min each) in 50 ml of PBS containing 0.1% Tween-20 and then incubated for 1 h with anti-rabbit or anti-goat immunoglobulin–horseradish peroxidase conjugate (dilution, 1:10.000). Before chemiluminescent detection the washing step was repeated. The membrane was developed with the ECL-Plus Western blotting detection system (Amersham/Pharmacia, Freiburg, Germany) and analyzed with a Lumi-Imager (Roche Diagnostics). For reprobing with another antibody, membranes were stripped of bound antibodies by incubation in 100 mM 2-mercaptoethanol, 2% sodium dodecyl sulfate, 62.5 mM Tris–HCl, pH 6.7, at 50 °C for 30 min with gentle agitation. After washing twice (10 min each) with PBS containing 0.1% Tween-20, membranes were again blocked in 5% nonfat dry milk in PBS for 1 h at room temperature. The second immunodetection was performed as outlined above.

Data analysis. All data are expressed as means ± SD. Statistical analysis was performed using SPSS 12.0 software. Statistical significance was determined by the Mann–Whitney test. A $p < 0.05$ was considered as statistically significant.

Results

Whole plasma lipid analysis

The distribution of plasma lipid species in Cav-1(−/−) mice and their wild-type littermates was analyzed after feeding with either with a low fat chow diet containing 10% kcal% fat or with a high fat diet containing 60% kcal% fat. Plasma samples were drawn from the same mice under fasting and post-prandial conditions. ESI-MS/MS analysis was performed with samples from 3 to 10 mice of each group. The results of whole plasma analysis are shown in Table 1.

The most abundant lipid class detected was CE. Significant changes between the genotypes were only detected for CE, free cholesterol, and phosphatidylcholine (PC) in fasted female mice fed with low fat diet and in post-prandial female mice on high fat diet for lysophosphatidylcholine (LPC). Ceramide and hexosylceramide were found at very low plasma levels. Ceramide was increased in fasted Cav-1(−/−) mice, and hexosylceramide concentrations

Table 1
Concentration of serum lipids in Cav-1(+/+) and Cav-1(−/−) mice

Lipid	Gender	Diet	Fasting	Serum concentration (μM)	
				Cav-1(+/+)	Cav-1(−/−)
Cholesteryl Ester	Male	Low fat	Fasted	3812 ± 1955	4753 ± 367
	Female	Low fat	Fasted	2852 ± 731	4166 ± 1227[a]
	Male	High fat	Fasted	5162 ± 2264	6006 ± 881
	Female	High fat	Fasted	3902 ± 1023	4691 ± 1211
	Male	Low fat	Post-prandial	3080 ± 1288	3877 ± 301
	Female	Low fat	Post-prandial	2671 ± 744	3250 ± 768
	Male	High fat	Post-prandial	5169 ± 2157	5909 ± 833
	Female	High fat	Post-prandial	4025 ± 848	5298 ± 1751
Free cholesterol	Male	Low fat	Fasted	367 ± 213	698 ± 148
	Female	Low fat	Fasted	372 ± 75	599 ± 143[a]
	Male	High fat	Fasted	780 ± 330	958 ± 191
	Female	High fat	Fasted	602 ± 196	758 ± 156
	Male	Low fat	Post-prandial	755 ± 402	996 ± 98
	Female	Low fat	Post-prandial	1388 ± 451	1782 ± 344
	Male	High fat	Post-prandial	716 ± 247	782 ± 171
	Female	High fat	Post-prandial	1083 ± 267	1147 ± 409
Phosphatidylcholine	Male	Low fat	Fasted	1443 ± 584	1898 ± 242
	Female	Low fat	Fasted	1046 ± 246	1476 ± 235[a]
	Male	High fat	Fasted	1849 ± 677	2349 ± 327
	Female	High fat	Fasted	1342 ± 396	1645 ± 288
	Male	Low fat	Post-prandial	2182 ± 1000	2723 ± 175
	Female	Low fat	Post-prandial	1494 ± 444	1897 ± 397
	Male	High fat	Post-prandial	2984 ± 1188	4166 ± 526
	Female	High fat	Post-prandial	2410 ± 452	3081 ± 1000
Lysophosphatidylcholine	Male	Low fat	Fasted	728 ± 283	864 ± 162
	Female	Low fat	Fasted	507 ± 106	568 ± 87
	Male	High fat	Fasted	721 ± 266	806 ± 122
	Female	High fat	Fasted	499 ± 129	525 ± 121
	Male	Low fat	Post-prandial	695 ± 184	813 ± 27
	Female	Low fat	Post-prandial	519 ± 68	582 ± 107
	Male	High fat	Post-prandial	807 ± 289	973 ± 113
	Female	High fat	Post-prandial	693 ± 57	956 ± 322[a]
Sphingomyelin	Male	Low fat	Fasted	177 ± 69	203 ± 20
	Female	Low fat	Fasted	118 ± 33	148 ± 27
	Male	High fat	Fasted	249 ± 74	311 ± 36
	Female	High fat	fasted	205 ± 53	240 ± 24
	Male	Low fat	Post-prandial	183 ± 61	217 ± 19
	Female	Low fat	Post-prandial	140 ± 40	166 ± 31
	Male	High fat	Post-prandial	321 ± 93	373 ± 50
	Female	High fat	Post-prandial	268 ± 64	297 ± 89
Ceramide	Male	Low fat	Fasted	3.4 ± 0.9	4.6 ± 0.1[a]
	Female	Low fat	Fasted	3.0 ± 0.5	4.3 ± 0.8[b]
	Male	High fat	Fasted	4.9 ± 1.7	5.5 ± 0.7
	Female	High fat	Fasted	3.2 ± 0.7	4.3 ± 1.2[a]
	Male	Low fat	Post-prandial	5.0 ± 1.6	6.8 ± 0.2
	Female	Low fat	Post-prandial	4.7 ± 1.4	5.8 ± 1.7
	Male	High fat	Post-prandial	7.0 ± 2.3	11.6 ± 2.5[a]
	Female	High fat	Post-prandial	5.1 ± 1.9	5.9 ± 2.0
Hexosylceramide	Male	Low fat	Fasted	2.3 ± 0.5	3.0 ± 1.1
	Female	Low fat	Fasted	1.9 ± 0.4	2.5 ± 0.5
	Male	High fat	Fasted	2.0 ± 0.6	1.9 ± 0.3
	Female	High fat	Fasted	1.8 ± 0.4	2.4 ± 0.3[a]
	Male	Low fat	Post-prandial	2.6 ± 0.7	4.2 ± 0.1[a]
	Female	Low fat	Post-prandial	1.9 ± 0.4	2.8 ± 0.6[b]
	Male	High fat	Post-prandial	2.7 ± 0.4	3.7 ± 0.5[a]
	Female	High fat	Post-prandial	2.5 ± 0.3	3.7 ± 1.4[a]

Data are presented as means ± SD of 3–10 mice per group.
[a] Significant difference ($p < 0.05$) between Cav-1(+/+) and Cav-1(−/−) mice.
[b] Significant difference ($p < 0.001$) between Cav-1(+/+) and Cav-1(−/−) mice.

were higher in post-prandial Cav-1(−/−) mice under both diets.

We next addressed the question if the distribution of lipid species, in particular in CE, was altered in Cav-1 deficiency. Since in mice acyl coenzyme A: cholesteryl acyltransferase activity (ACAT) prefers saturated and monounsaturated fatty acids for esterification, whereas lecithin-cholesterol acyltransferase (LCAT) prefers polyunsaturated fatty acids we compared the distribution of saturated and monounsaturated with polyunsaturated fatty acids in CE by calculating the ratio of saturated + monounsaturated on polyunsaturated CE. In fasting plasma of Cav-1(−/−) mice on low fat diet we detected a significant increase of this ratio (0.36 ± 0.05 vs. 0.60 ± 0.10 and 0.58 ± 0.15 vs. 0.82 ± 0.23, respectively) (Fig. 1A). Further analysis revealed in male mice increased proportions of CE16:1 ($8.1\% \pm 1.9\%$ vs. $12.4\% \pm 0.9\%$), CE18:1 ($13.5\% \pm 2.0\%$ vs. $20.4\% \pm 2.9\%$), and CE20:3 ($6.1\% \pm 0.7\%$ vs. $8.3\% \pm 0.5\%$) while the percentage of CE18:2 ($19.1\% \pm 2.0\%$ vs. $14.5\% \pm 1.3\%$) and CE22:6 ($5.1\% \pm 0.4\%$ vs. $3.7\% \pm 0.1\%$) was decreased in Cav-1 deficiency (Fig. 1B). Similar results were obtained in female mice. Increased proportions were detected for CE16:1 ($10.7\% \pm 1.7\%$ vs. $12.3\% \pm 1.4\%$) and CE18:1 ($19.7\% \pm 4.4\%$ vs. $25.9\% \pm 5.3\%$) and decreased levels were found for CE18:2 ($16.2\% \pm 1.3\%$ vs. $12.4\% \pm 2.6\%$) and CE22:6 ($4.5\% \pm 0.5\%$ vs. $3.7\% \pm 0.5\%$).

Analysis of lipoprotein subfractions

We next addressed the question if the observed changes in lipids and lipid species in whole plasma in Cav-1 defi-

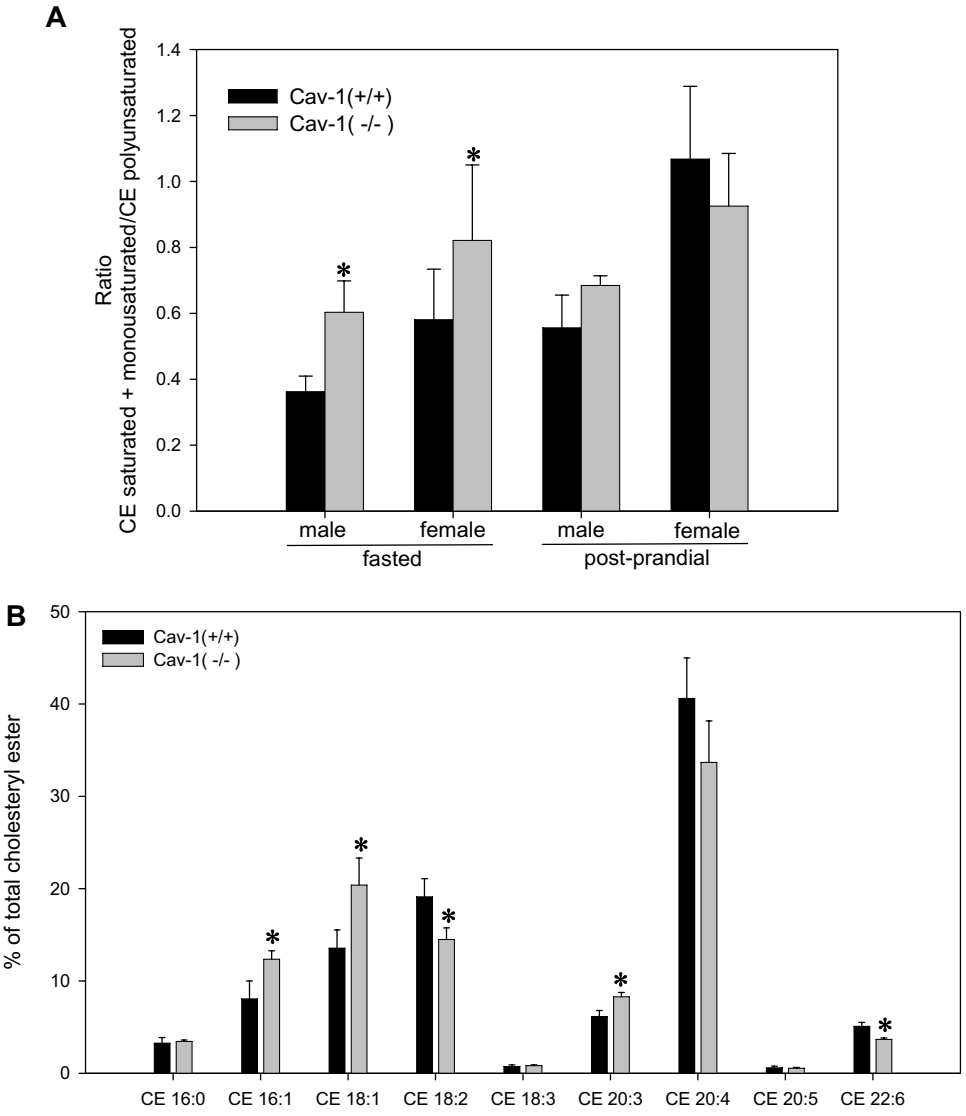

Fig. 1. The distribution of cholesterol ester species is altered in Cav-1 deficiency. Plasma samples were taken from 9 month old Cav-1 and wild-type mice that were kept on a low fat diet (10% kcal% fat) and analyzed by mass spectrometry as described in Material and methods. (A) The ratio saturated + monounsaturated/polyunsaturated CE was calculated form analysis of single CE species. Data are expressed as means ± SD (3–10 mice per group). $^{*}p < 0.05$ Cav-1(−/−) vs. Cav-1(+/+). (B) Data are presented as percentage of total CE and are expressed as means ± SD (6 Cav-1(+/+) mice and 3 Cav-1(−/−). $^{*}p < 0.05$ Cav-1(−/−) vs. Cav-1(+/+).

ciency were accompanied by alterations in lipoprotein distribution. Size-exclusion chromatography (FPLC) was utilized to fractionate plasma lipoproteins from pooled samples of male Cav-1(−/−) and Cav-1(+/+) mice on low fat and high fat diet.

As published previously [16], we detected a considerable increase in triglycerides within the chylomicrons/VLDL fraction that was even pronounced under high fat diet (Fig. 2C). Slightly increased HDL-CE levels were detected independent of diet (Fig. 2A). Moreover, when mice were challenged with the high fat diet we observed a shift to larger HDL particles that was markedly pronounced in Cav-1(−/−) mice compared to their wild-type littermates (Fig. 2A and B).

Agarose gel electrophoresis and immunoblotting with apo-AI

The observed enhanced shift to larger HDL particles in Cav-1(−/−) mice was further investigated by analyzing the distribution of apo-AI containing HDL particles in the different genotypes. For this analysis pooled whole plasma samples of the male Cav-1(−/−) and Cav-1(+/+) mice on low fat and high fat diet were subjected to agarose gel electrophoresis and immunoblotting against apo-AI. Post-prandial samples as well as fasting samples from the same mice were used.

In accordance with the data from FPLC analysis, no major difference in the distribution of HDL subclasses was observed when mice were kept on low fat diet. The same was found for fasting plasma in high fat diet fed mice. In contrast, when post-prandial plasma was taken from mice fed with high fat diet, Cav-1(−/−) mice showed a markedly increased pre-β-HDL fraction. In addition, a shift from immature slow migrating to mature fast migrating apo-AI containing α-HDL particles was observed (Fig. 3).

Two-dimensional nondenaturing gradient gel electrophoresis

Since slow and fast migrating HDL differ in their apolipoprotein composition and, in particular in apoE content which is predominantly found in slow migrating HDL particles, the distribution of apo-AI and apoE containing particles was analyzed in fasting and post-prandial plasma of the high fat diet fed male mice by 2 D gradient gel electrophoresis (2D-GGE).

Corresponding to one dimensional native agarose gel electrophoresis the increase in pre-β-HDL in Cav-1(−/−) mice can also be observed in the 2D-GGE. In comparison to fasting plasma, post-prandial samples exhibit an increase in apo-AI containing α-HDL in both genotypes. However, this increase is considerably higher in Cav-1(−/−) mice. Cav-1(−/−) mice showed an expansion of apoE containing HDL particles in response to high fat diet, whereas in wild-type mice no significant response of apoE containing particles to high fat diet was found. As a consequence of these findings a partial colocalization of apo-AI and apoE containing particles could be observed in the plasma of post-prandial knockout mice while this was not apparent in Cav-1(+/+) mice (Fig. 4).

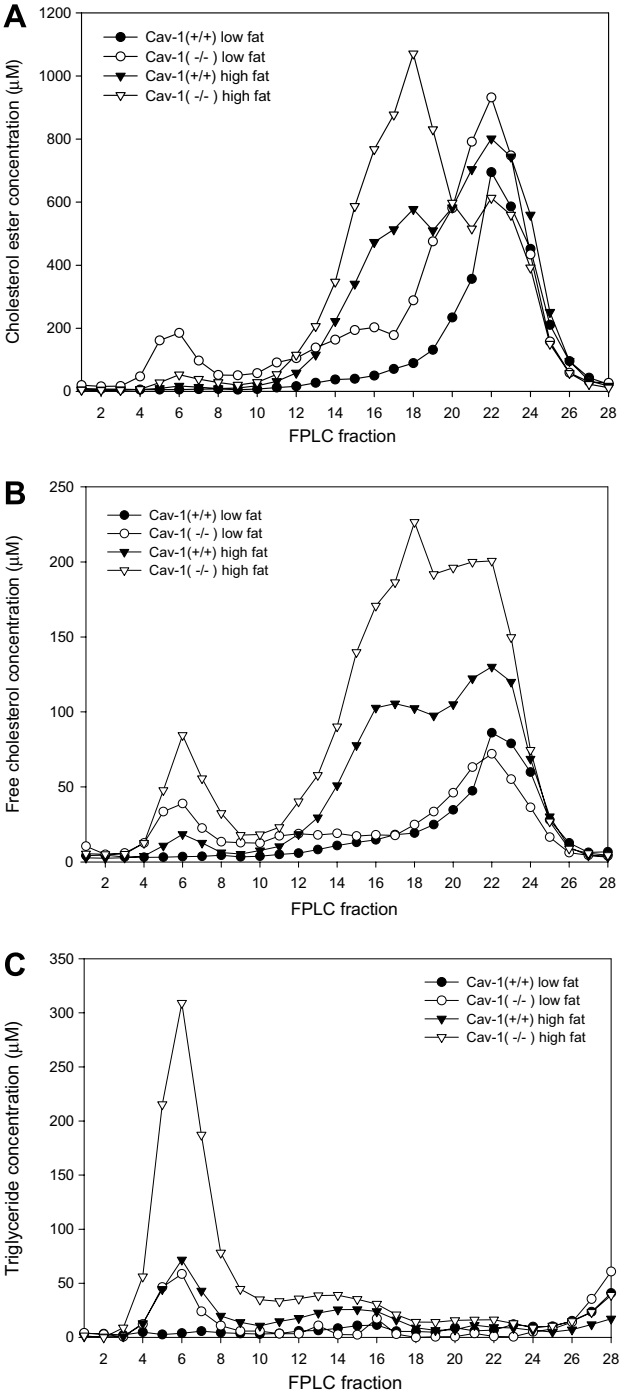

Fig. 2. Plasma HDL-CE (A), HDL free cholesterol (B) and VLDL/chylomicron triglyceride (C) concentrations are increased in Cav-1 deficiency under high fat diet. Plasma was taken post-prandial from male mice that were fed with low fat (10% kcal% fat) or high fat diet (60% kcal% fat). Samples of 5–6 mice of each group were pooled and 50 µl per pool were subjected to FPLC fractionation followed by mass spectrometry analysis as described in Material and methods.

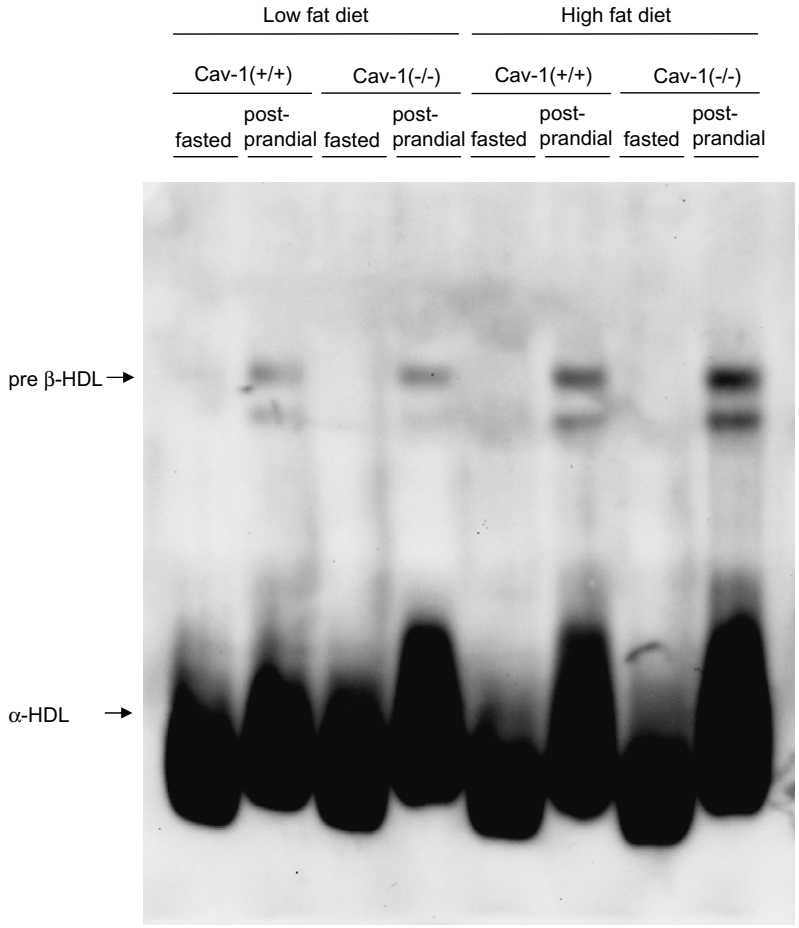

Fig. 3. Cav-1(−/−) mice reveal increased pre-β-HDL fraction and a shift from slow to fast migrating α-HDL. Plasma was taken post-prandial or after 14 h of fasting from 9-month-old male mice that were fed with low fat (10% kcal% fat) or high fat diet (60% kcal% fat). Samples of 3–8 mice of each group were pooled and 5 μl plasma per pool were separated by agarose gel electrophoresis and immunoblotted with anti-apo-AI as described in Material and methods.

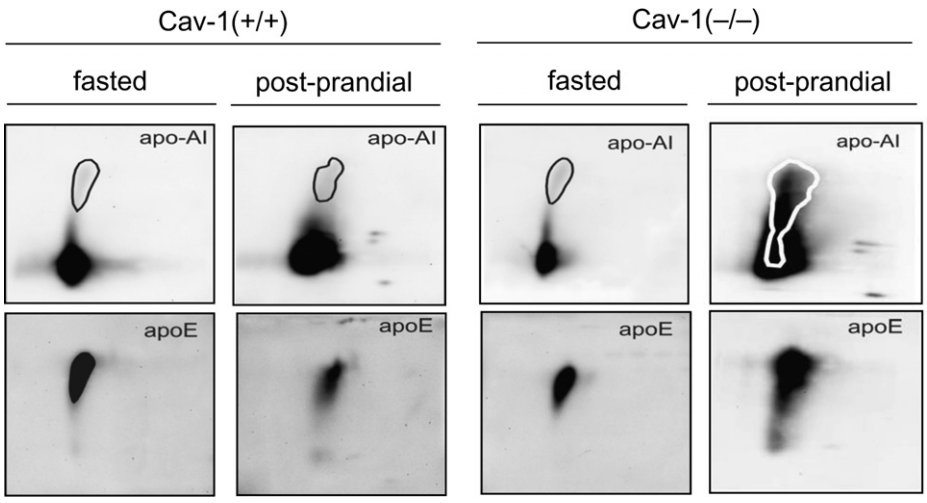

Fig. 4. The apoE containing HDL fraction is post-prandial increased Cav-1(−/−) mice on high fat diet. Plasma was taken post-prandial or after 14 h of fasting from 9-month-old male mice that were fed with high fat diet (60% kcal% fat). Samples of 5–8 mice of each group were pooled and 5 μl plasma subjected to 2D-GGE and immunoblotting with anti-apo-AI and anti-apoE as described in Material and methods. The circled areas on the blot represent the immunoreactivity of apo-AI on the same blot.

Discussion

In the present study, we performed a detailed serum lipid and lipoprotein analysis of Cav-1 deficient and wild-type mice using mass spectrometry, FPLC and immunoblotting methods to get further insights into the role of Cav-1 in lipid metabolism.

In whole plasma samples, we detected significant increases in ceramide and hexosylceramide in Cav-1 deficiency upon dietary challenge in a number of feeding groups. It seems unlikely that this shift is caused by enhanced activity, expression or secretion of sphigomyelinase, since plasma sphingomyelin concentrations were not altered in both genotypes.

In contrast, analysis of lipid species revealed striking alterations in the distribution of CE species in Cav-1 deficiency. These effects are probably due to enhanced ACAT2 activity. Plasma samples of ACAT2(−/−)/LDL receptor(−/−) mice reveal decreased saturated + monounsaturated on polyunsaturated fatty acid ratio in CE in comparison to ACAT2(+/+)/LDL receptor(−/−) mice [24] indicating that increased ratios could be expected in enhanced ACAT2 activity. Moreover, the CE species profile detected in plasma of ACAT2(−/−)/ApoE(−/−) mice displays an almost opposite composition to the profile of Cav-1(−/−) mice [25]. While we found increased proportions in CE16:1, CE18:1, and CE20:3, these CE species were significantly decreased in ACAT2 deficiency. Vice versa CE22:6 that is decreased in Cav-1 deficiency was increased ACAT2 deficiency. Indeed, enhanced ACAT activity has recently been described in Cav-1(−/−) mouse embryonic fibroblasts [26]. Since Cav-1 may mediate the transfer of newly synthesized cholesterol from the endoplasmatic reticulum to the plasma membrane [27], it has been suggested that Cav-1 deficiency would be associated with the accumulation of cholesterol in the endoplasmatic reticulum resulting in increased ACAT activity and reduced free cholesterol synthesis [26]. However, since controversial data on Cav-1 expression in hepatocytes do exist [28,29], alternative, indirect mechanisms may be involved. Since ACAT2 generates CE for newly secreted VLDL in mice [30], the highly increased chylomicron/VLDL fraction in Cav-1(−/−) may also relate to increased ACAT2 activity in addition to the previously discussed inability to rapidly clear orally administered fat load [16].

Alterations in HDL lipoprotein size and composition were predominantly detected in post-prandial samples under high fat diet. In these mice, an increase in HDL-CE and free cholesterol accompanied by an increased pre-β-HDL fraction, a shift to fast migrating α-HDL and, most strikingly in post-prandial animals, an increase in the apoE containing HDL fraction was observed. Increased apoE-rich HDL-cholesterol has been described under various conditions including LCAT deficiency [31]. However, since Cav-1(−/−) mice show increased amounts of HDL-CE, reduced LCAT activity is not plausible. More likely, the increase in HDL-CE and apoE-rich HDL may reflect impaired SR-BI mediated HDL uptake. Within the plasma membrane caveolae appear to be the site of SR-BI dependent CE uptake from HDL [32]. Cav-1 expression induces the formation of SR-BI dimers in HepG2 cells thereby increasing selective CE uptake from HDL [33]. In addition, the uptake of spherical apoE-rich HDL is suggested to be mediated by SR-BI [34], strongly indicating that the alterations in HDL-cholesterol concentration and composition in Cav-1 deficient mice are caused by impaired SR-BI function.

In summary, using different feeding and plasma sampling strategies we here provided a comprehensive set of plasma lipid and lipoprotein data from Cav-1 deficient mice that highlight the role of Cav-1 in lipid metabolism. Expanding previously published data that only could show Cav-1 dependent effects on the VLDL/chylomicron fraction [16], we could demonstrate an additional striking role of Cav-1 in HDL-cholesterol metabolism. Our results probably reflect a variety of Cav-1 functions including differential apo-AI/apoE distribution and modulation of ACAT activity and SR-BI function. However, more detailed functional data will be needed to further elucidate the mechanisms by which cellular Cav-1 dependent pathways interact with lipoprotein metabolism at the molecular level.

Acknowledgments

We thank Doreen Müller and Jolante Aiwanger for excellent technical assistance. This work was supported by Deutsche Forschungsgemeinschaft (Transregio SFB-TR 13).

References

[1] R. Hnasko, M.P. Lisanti, The biology of caveolae: lessons from caveolin knockout mice and implications for human disease, Mol. Interv. 3 (2003) 445–464.
[2] A.M. Fra, E. Williamson, K. Simons, R.G. Parton, De novo formation of caveolae in lymphocytes by expression of VIP21-caveolin, Proc. Natl. Acad. Sci. USA 92 (1995) 8655–8659.
[3] K.G. Rothberg, J.E. Heuser, W.C. Donzell, Y.S. Ying, J.R. Glenney, R.G. Anderson, Caveolin, a protein component of caveolae membrane coats, Cell 68 (1992) 673–682.
[4] M. Murata, J. Peranen, R. Schreiner, F. Wieland, T.V. Kurzchalia, K. Simons, VIP21/caveolin is a cholesterol-binding protein, Proc. Natl. Acad. Sci. USA 92 (1995) 10339–10343.
[5] L.S. Le, T.V. Kurzchalia, Getting rid of caveolins: phenotypes of caveolin-deficient animals, Biochim. Biophys. Acta 1746 (2005) 322–333.
[6] M. Drab, P. Verkade, M. Elger, M. Kasper, M. Lohn, B. Lauterbach, J. Menne, C. Lindschau, F. Mende, F.C. Luft, A. Schedl, H. Haller, T.V. Kurzchalia, Loss of caveolae, vascular dysfunction, and pulmonary defects in caveolin-1 gene-disrupted mice, Science 293 (2001) 2449–2452.
[7] F. Galbiati, J.A. Engelman, D. Volonte, X.L. Zhang, C. Minetti, M. Li, H. Hou Jr., B. Kneitz, W. Edelmann, M.P. Lisanti, Caveolin-3 null mice show a loss of caveolae, changes in the microdomain distribution of the dystrophin–glycoprotein complex, and t-tubule abnormalities, J. Biol. Chem. 276 (2001) 21425–21433.

[8] B. Razani, X.B. Wang, J.A. Engelman, M. Battista, G. Lagaud, X.L. Zhang, B. Kneitz, H. Hou Jr., G.J. Christ, W. Edelmann, M.P. Lisanti, Caveolin-2-deficient mice show evidence of severe pulmonary dysfunction without disruption of caveolae, Mol. Cell Biol. 22 (2002) 2329–2344.
[9] C.D. Hardin, J. Vallejo, Caveolins in vascular smooth muscle: form organizing function, Cardiovasc. Res. 69 (2006) 808–815.
[10] W. Schubert, P.G. Frank, S.E. Woodman, H. Hyogo, D.E. Cohen, C.W. Chow, M.P. Lisanti, Microvascular hyperpermeability in caveolin-1(−/−) knock-out mice. Treatment with a specific nitric-oxide synthase inhibitor, L-NAME, restores normal microvascular permeability in Cav-1 null mice, J. Biol. Chem. 277 (2002) 40091–40098.
[11] P.E. Scherer, M.P. Lisanti, G. Baldini, M. Sargiacomo, C.C. Mastick, H.F. Lodish, Induction of caveolin during adipogenesis and association of GLUT4 with caveolin-rich vesicles, J. Cell Biol. 127 (1994) 1233–1243.
[12] A.G. Ostermeyer, J.M. Paci, Y. Zeng, D.M. Lublin, S. Munro, D.A. Brown, Accumulation of caveolin in the endoplasmic reticulum redirects the protein to lipid storage droplets, J. Cell Biol. 152 (2001) 1071–1078.
[13] L.S. Le, E. Hajduch, M.R. Lindsay, L. Le, X.C. Thiele, P. Ferre, R.G. Parton, T. Kurzchalia, K. Simons, I. Dugail, Cholesterol-induced caveolin targeting to lipid droplets in adipocytes: a role for caveolar endocytosis, Traffic 7 (2006) 549–561.
[14] D.A. Bernlohr, N.R. Coe, V.J. LiCata, Fatty acid trafficking in the adipocyte, Semin. Cell Dev. Biol. 10 (1999) 43–49.
[15] A. Ring, L.S. Le, J. Pohl, P. Verkade, W. Stremmel, Caveolin-1 is required for fatty acid translocase (FAT/CD36) localization and function at the plasma membrane of mouse embryonic fibroblasts, Biochim. Biophys. Acta 1761 (2006) 416–423.
[16] B. Razani, T.P. Combs, X.B. Wang, P.G. Frank, D.S. Park, R.G. Russell, M. Li, B. Tang, L.A. Jelicks, P.E. Scherer, M.P. Lisanti, Caveolin-1-deficient mice are lean, resistant to diet-induced obesity, and show hypertriglyceridemia with adipocyte abnormalities, J. Biol. Chem. 277 (2002) 8635–8647.
[17] B. Razani, J.A. Engelman, X.B. Wang, W. Schubert, X.L. Zhang, C.B. Marks, F. Macaluso, R.G. Russell, M. Li, R.G. Pestell, V.D. Di, H. Hou Jr., B. Kneitz, G. Lagaud, G.J. Christ, W. Edelmann, M.P. Lisanti, Caveolin-1 null mice are viable but show evidence of hyperproliferative and vascular abnormalities, J. Biol. Chem. 276 (2001) 38121–38138.
[18] B. Brugger, G. Erben, R. Sandhoff, F.T. Wieland, W.D. Lehmann, Quantitative analysis of biological membrane lipids at the low picomole level by nano-electrospray ionization tandem mass spectrometry, Proc. Natl. Acad. Sci. USA 94 (1997) 2339–2344.
[19] G. Liebisch, W. Drobnik, M. Reil, B. Trumbach, R. Arnecke, B. Olgemoller, A. Roscher, G. Schmitz, Quantitative measurement of different ceramide species from crude cellular extracts by electrospray ionization tandem mass spectrometry (ESI-MS/MS), J. Lipid Res. 40 (1999) 1539–1546.
[20] G. Liebisch, W. Drobnik, B. Lieser, G. Schmitz, High-throughput quantification of lysophosphatidylcholine by electrospray ionization tandem mass spectrometry, Clin. Chem. 48 (2002) 2217–2224.
[21] G. Liebisch, B. Lieser, J. Rathenberg, W. Drobnik, G. Schmitz, High-throughput quantification of phosphatidylcholine and sphingomyelin by electrospray ionization tandem mass spectrometry coupled with isotope correction algorithm, Biochim. Biophys. Acta 1686 (2004) 108–117.
[22] G. Liebisch, M. Binder, R. Schifferer, T. Langmann, B. Schulz, G. Schmitz, High throughput quantification of cholesterol and cholesteryl ester by electrospray ionization tandem mass spectrometry (ESI-MS/MS), Biochim. Biophys. Acta 1761 (2006) 121–128.
[23] W. Innis-Whitehouse, X. Li, W.V. Brown, N.A. Le, An efficient chromatographic system for lipoprotein fractionation using whole plasma, J. Lipid Res. 39 (1998) 679–690.
[24] R.G. Lee, K.L. Kelley, J.K. Sawyer, R.V. Farese Jr., J.S. Parks, L.L. Rudel, Plasma cholesteryl esters provided by lecithin:cholesterol acyltransferase and acyl-coenzyme a:cholesterol acyltransferase 2 have opposite atherosclerotic potential, Circ. Res. 95 (2004) 998–1004.
[25] E.L. Willner, B. Tow, K.K. Buhman, M. Wilson, D.A. Sanan, L.L. Rudel, R.V. Farese Jr., Deficiency of acyl CoA:cholesterol acyltransferase 2 prevents atherosclerosis in apolipoprotein E-deficient mice, Proc. Natl. Acad. Sci. USA 100 (2003) 1262–1267.
[26] P.G. Frank, M.W. Cheung, S. Pavlides, G. Llaverias, D.S. Park, M.P. Lisanti, Caveolin-1 and regulation of cellular cholesterol homeostasis, Am. J. Physiol Heart Circ. Physiol 291 (2006) H677–H686.
[27] E.J. Smart, Y. Ying, W.C. Donzell, R.G. Anderson, A role for caveolin in transport of cholesterol from endoplasmic reticulum to plasma membrane, J. Biol. Chem. 271 (1996) 29427–29435.
[28] L. Malerod, K. Juvet, T. Gjoen, T. Berg, The expression of scavenger receptor class B, type I (SR-BI) and caveolin-1 in parenchymal and nonparenchymal liver cells, Cell Tissue Res. 307 (2002) 173–180.
[29] M. Moreno, H. Molina, L. Amigo, S. Zanlungo, M. Arrese, A. Rigotti, J.F. Miquel, Hepatic overexpression of caveolins increases bile salt secretion in mice, Hepatology 38 (2003) 1477–1488.
[30] R.G. Lee, R. Shah, J.K. Sawyer, R.L. Hamilton, J.S. Parks, L.L. Rudel, ACAT2 contributes cholesteryl esters to newly secreted VLDL, whereas LCAT adds cholesteryl ester to LDL in mice, J. Lipid Res. 46 (2005) 1205–1212.
[31] C.D. Mitchell, W.C. King, K.R. Applegate, T. Forte, J.A. Glomset, K.R. Norum, E. Gjone, Characterization of apolipoprotein E-rich high density lipoproteins in familial lecithin:cholesterol acyltransferase deficiency, J. Lipid Res. 21 (1980) 625–634.
[32] G.A. Graf, S.V. Matveev, E.J. Smart, Class B scavenger receptors, caveolae and cholesterol homeostasis, Trends Cardiovasc. Med. 9 (1999) 221–225.
[33] T.Q. Truong, D. Aubin, P. Bourgeois, L. Falstrault, L. Brissette, Opposite effect of caveolin-1 in the metabolism of high-density and low-density lipoproteins, Biochim. Biophys. Acta 1761 (2006) 24–36.
[34] K.E. Kypreos, V.I. Zannis, Pathway of biogenesis of apolipoprotein E-containing HDL in vivo with the participation of ABCA1 and LCAT, Biochem. J. 403 (2007) 359–367.